

Measuring the Kerr spin parameter of regular black holes from their shadow

Zilong Li and Cosimo Bambi¹

Center for Field Theory and Particle Physics & Department of Physics,
Fudan University,
220 Handan Road, 200433 Shanghai, China

E-mail: zilongli@fudan.edu.cn, bambi@fudan.edu.cn

Abstract. In a previous paper, one of us has showed that, at least in some cases, the Kerr-nature of astrophysical black hole candidates is extremely difficult to test and current techniques, even in presence of excellent data not available today, cannot distinguish a Kerr black hole from a Bardeen one, despite the substantial difference of the two backgrounds. In this paper, we investigate if the detection of the “shadow” of nearby super-massive black hole candidates by near future mm/sub-mm very long baseline interferometry experiments can do the job. More specifically, we consider the measurement of the Kerr spin parameter of the Bardeen and Hayward regular black holes from their shadow, and we then compare the result with the estimate inferred from the $K\alpha$ iron line and from the frequency of the innermost stable circular orbit. For non-rotating black holes, the shadow approach provides different values, and therefore the Kerr black hole hypothesis can potentially be tested. For near extremal objects, all the approaches give quite similar results, and therefore it is not possible to constrain deviations from the Kerr solution. The present work confirms that it is definitively challenging to test this kind of metrics, even with future facilities. However, the detection of a source that looks like a fast-rotating Kerr black hole can put meaningful constraints on the nature of the compact object.

Keywords: gravity, modified gravity, astrophysical black holes.

¹Corresponding author

Contents

1	Introduction	1
2	Testing the Kerr-nature of black hole candidates	3
3	Black hole’s shadow	4
4	Measuring the Kerr spin parameter from the black hole’s shadow	7
5	Discussion	10
6	Summary and conclusions	15

1 Introduction

In 4-dimensional general relativity, uncharged black holes (BHs) are described by the Kerr solution and are completely specified by two parameters, the mass M and the spin angular momentum J [1–3]. The condition for the existence of the event horizon is $|a_*| \leq 1$, where $a_* = a/M = J/M^2$ is the spin parameter¹. Astrophysical BHs, if they exist, are expected to be well described by the Kerr metric: initial deviations from the Kerr geometry should be quickly radiated away through the emission of gravitational waves [4, 5], an initially non-vanishing electric charge would be shortly neutralized in their highly ionized environment [6], while the presence of the accretion disk is completely negligible in most cases. Astrophysical BH candidates are dark compact objects in X-ray binary systems with a mass $M \approx 5 - 20 M_\odot$ and super-massive bodies in galactic nuclei with a mass $M \sim 10^5 - 10^9 M_\odot$ [7]. They are thought to be the Kerr BHs of general relativity, but their actual nature is still to be verified. Stellar-mass BH candidates are simply too heavy to be neutron or quark stars for any plausible matter equation of state [8, 9]. At least some of the super-massive BH candidates at the centers of galaxies are too massive, compact, and old to be clusters of non-luminous bodies [10]. The non-observation of electromagnetic radiation emitted by the possible surface of these objects may also be interpreted as an indication for the existence of an event horizon [11, 12] (but see [13, 14]). However, there is no evidence that the spacetime geometry around them is really described by the Kerr solution.

The possibility of testing the nature of astrophysical BH candidates with current and near future observations has recently become a quite active research field (for a review, see [15, 16]). Today, there are two relatively robust techniques to estimate the spin parameter of BH candidates under the assumption that the geometry around them is described by the Kerr metric: the so-called continuum-fitting method [17–19] and the analysis of the $K\alpha$ iron line [20–22]. Both the approaches can be used to probe the geometry of the spacetime around BH candidates and measure the spin parameter and possible deviations from the Kerr solution [23–30]. However, it turns out that there is a strong correlation between the spin and possible deformations and that one can only constrain a certain combination of these quantities. In other words, the thermal spectrum of a thin accretion disk and the profile of the $K\alpha$ iron line of a Kerr BH with spin parameter a_* can be extremely similar

¹Throughout the paper, we use units in which $G_N = c = 1$, unless stated otherwise.

– practically indistinguishable – from the ones of non-Kerr compact objects with different spin parameters. In Ref. [31], one of us has showed that, at least for some non-Kerr metrics, the combination of the continuum-fitting method and of the iron line analysis cannot fix this problem. Other approaches to test the nature of BH candidates are either not yet mature, like the case of quasi-periodic oscillations [32, 33], or it is not clear when astrophysical data will be available, like the case of gravitational waves or observations of a BH binary with a pulsar companion [34–40]. The estimate of the power of steady and transient jets can potentially break the degeneracy between spin parameter and deviations from the Kerr solution [41, 42], but at present we do not know the exact mechanism responsible for these phenomena. A rough estimate of possible deviations from the Kerr geometry in the spacetime around super-massive BH candidates can be obtained from considerations on their radiative efficiency and on the possible mechanisms capable of spinning them up and down [43–46].

A quite promising technique to test the nature of super-massive BH candidates with near future very long baseline interferometry (VLBI) facilities is through the observation of the “shadow” of these objects [47, 48]. The shadow is a dark area over a bright background appearing in the image of an optically thin emitting region around a BH [49–51]. While the intensity map of the image depends on the details of the accretion process and of the emission mechanisms, the boundary of the shadow is only determined by the metric of the spacetime, since it corresponds to the apparent image of the photon capture sphere as seen by a distant observer. The possibility of testing the nature of supermassive BH candidates by observing the shape of their shadow has been already discussed in the literature, starting from Ref. [52, 53]. In general, very accurate observations are necessary, because the effect of possible deviations from the Kerr solution are tiny [54–60].

At first approximation, the shape of the shadow of a BH is a circle. The radius of the circle corresponds to the apparent photon capture radius, which, for a given metric, is set by the mass of the compact object and its distance from us. These two quantities are usually known with a large uncertainty, and therefore the observation of the size of the shadow can unlikely be used to test the nature of the BH candidate (but see Ref. [60]). The shape of the shadow is instead the key-point. The first order correction to the circle is due to the BH spin, as the photon capture radius is different for co-rotating and counter-rotating particles. The boundary of the shadow has thus a dent on one side: the deformation is more pronounced for an observer on the equatorial plane (viewing angle $i = 90^\circ$) and decreases as the observer moves towards the spin axis, to completely disappear when $i = 0^\circ$ or 180° . Possible deviations from the Kerr solutions usually introduces smaller corrections.

In the present paper, we consider the measurement of the Kerr spin parameter of Kerr BHs and non-Kerr regular BHs; that is, we measure the spin parameter a_* from the shape of the shadow of a BH assuming it is of the Kerr kind. We use the procedure proposed in Ref. [61], which is based on the determination of the distortion parameter $\delta_s = D_{cs}/R_s$, where D_{cs} and R_s are, respectively, the dent and the radius of the shadow. In the case of non-Kerr BHs, this technique provides the correct value of a_* for non-rotating objects, but a quite different spin for near extremal states. We then compare these measurements with the ones we could infer from the analysis of the $K\alpha$ iron line and the observation of a hot spot orbiting around the BH candidate. The $K\alpha$ iron line approach is currently the only relatively robust technique to probe the spacetime geometry around these objects. The observations of hot spots orbiting around nearby super-massive BH candidates with mm/sub-mm VLBI facilities will hopefully allow to determine the frequency of test-particles at the innermost stable circular orbit (ISCO) radius. For non-rotating and slow-rotating objects, the

shadow approach provides different results with respect to the other two techniques, so that a possible combination of these methods may break the degeneracy between spin parameter and possible deviations from the Kerr solution. All the approaches seem instead to provide quite similar measurements for near extremal BHs, which means that their combination cannot be used to test the spacetime geometry around these objects. Our work confirms the difficulty to observationally test the Kerr nature of astrophysical BH candidates. Only very good observations of the shadow, which are capable of measuring simultaneously the spin and possible deformations from the Kerr solution, might be required to test the Kerr BH hypothesis. However, in the case of objects that look like very fast-rotating Kerr BHs, interesting constraints on their nature seem to be possible.

The content of the paper is as follows. In Section 2, we present our approach to test the nature of astrophysical BH candidates and we introduce the metrics that will be used in the rest of the paper. In Section 3, we briefly review the concept and the calculation of the BH's shadow. Section 4 is devoted to the measurement of the Kerr spin parameter: we apply the procedure proposed in Ref. [61] to measure the spin of a Kerr BH to the Bardeen and Hayward BHs. Such a prescription provides the correct value of the spin parameter for non-rotating objects, but a wrong estimate for fast-rotating BHs. The results are then compared with the measurements we would obtain from the analysis of the $K\alpha$ iron line and the hot spot model in Section 5. Summary and conclusions are in Section 6.

2 Testing the Kerr-nature of black hole candidates

In Boyer-Lindquist coordinates, the non-vanishing metric coefficients of the Kerr metric are

$$\begin{aligned} g_{tt} &= -\left(1 - \frac{2Mr}{\Sigma}\right), & g_{t\phi} &= -\frac{2aMr \sin^2 \theta}{\Sigma}, \\ g_{\phi\phi} &= \left(r^2 + a^2 + \frac{2a^2Mr \sin^2 \theta}{\Sigma}\right) \sin^2 \theta, & g_{rr} &= \frac{\Sigma}{\Delta}, & g_{\theta\theta} &= \Sigma, \end{aligned} \quad (2.1)$$

where

$$\Sigma = r^2 + a^2 \cos^2 \theta, \quad \Delta = r^2 - 2Mr + a^2. \quad (2.2)$$

M is the BH mass and $a = J/M$ is its spin parameter. If we want to test the Kerr nature of an astrophysical BH candidate, it is convenient to consider a more general spacetime, in which the central object is described by a mass M , spin parameter a , and one (or more) “deformation parameter(s)”. The latter measure possible deviations from the Kerr solution, which must be recovered when all the deformation parameters vanish. The strategy is thus to calculate some observables in this more general background and then fit the data of the source to find the allowed values of the spin and of the deformation parameters. If the observations require vanishing deformation parameters, the compact object is a Kerr BH. If they demand non-vanishing deformation parameters, astrophysical BH candidates are not the Kerr BH of general relativity and new physics is necessary. In general, however, the result is that observations allows both the possibility of a Kerr BH with a certain spin parameter and non-Kerr objects with different spin parameters.

As non-Kerr metrics, in the present work we will focus on the Bardeen and Hayward BHs [62, 63], which cannot be observationally tested by current techniques (continuum-fitting method and iron line analysis), even in presence of excellent data not available today [31].

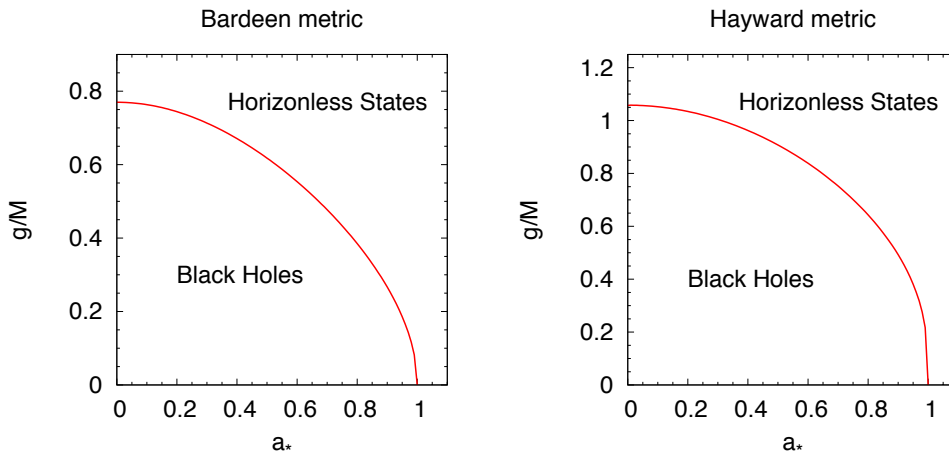


Figure 1. Rotating Bardeen (left panel) and Hayward (right panel) metrics. The red solid lines separate the regions with BHs from the ones with horizonless objects.

The rotating solutions have the same form of the Kerr metric, with the mass M replaced by m as follows [64, 65]:

$$M \rightarrow m_{\text{B}} = M \left(\frac{r^2}{r^2 + g^2} \right)^{3/2}, \quad (2.3)$$

$$M \rightarrow m_{\text{H}} = M \frac{r^3}{r^3 + g^3}. \quad (2.4)$$

g can be interpreted as the magnetic charge of a non-linear electromagnetic field or just as a quantity introducing a deviation from the Kerr metric and solving the central singularity. The position of the even horizon is given by the larger root of $\Delta = 0$ and therefore there is a bound on the maximum value of the spin parameter, above which there are no BHs. The maximum value of a_* is 1 for $g/M = 0$ (Kerr case), and decreases as g/M increases. The regions of BHs and horizonless states on the plane $(a_*, g/M)$ are shown in Fig. 1. In what follows, we will restrict the attention to the BH region: even if they can be created [65], the horizonless states are likely very unstable objects with a short lifetime due to the ergoregion instability.

3 Black hole's shadow

The shadow of a BH is a dark area over a bright background appearing in the image of an optically thin emitting region around the compact object. The boundary of the shadow depends only on the geometry of the background and turns out to correspond to the apparent image of the photon capture sphere as seen by a distant observer: if one fires a photon inside the boundary of the shadow, the photon is swallowed by the BH; if outside, the photon reaches a minimum distance from the compact object and then comes back to infinity. In this section, we will briefly review the study of the shadow of a BH (for more details, see e.g. Sec. 63 of [49] or Ref. [66]).

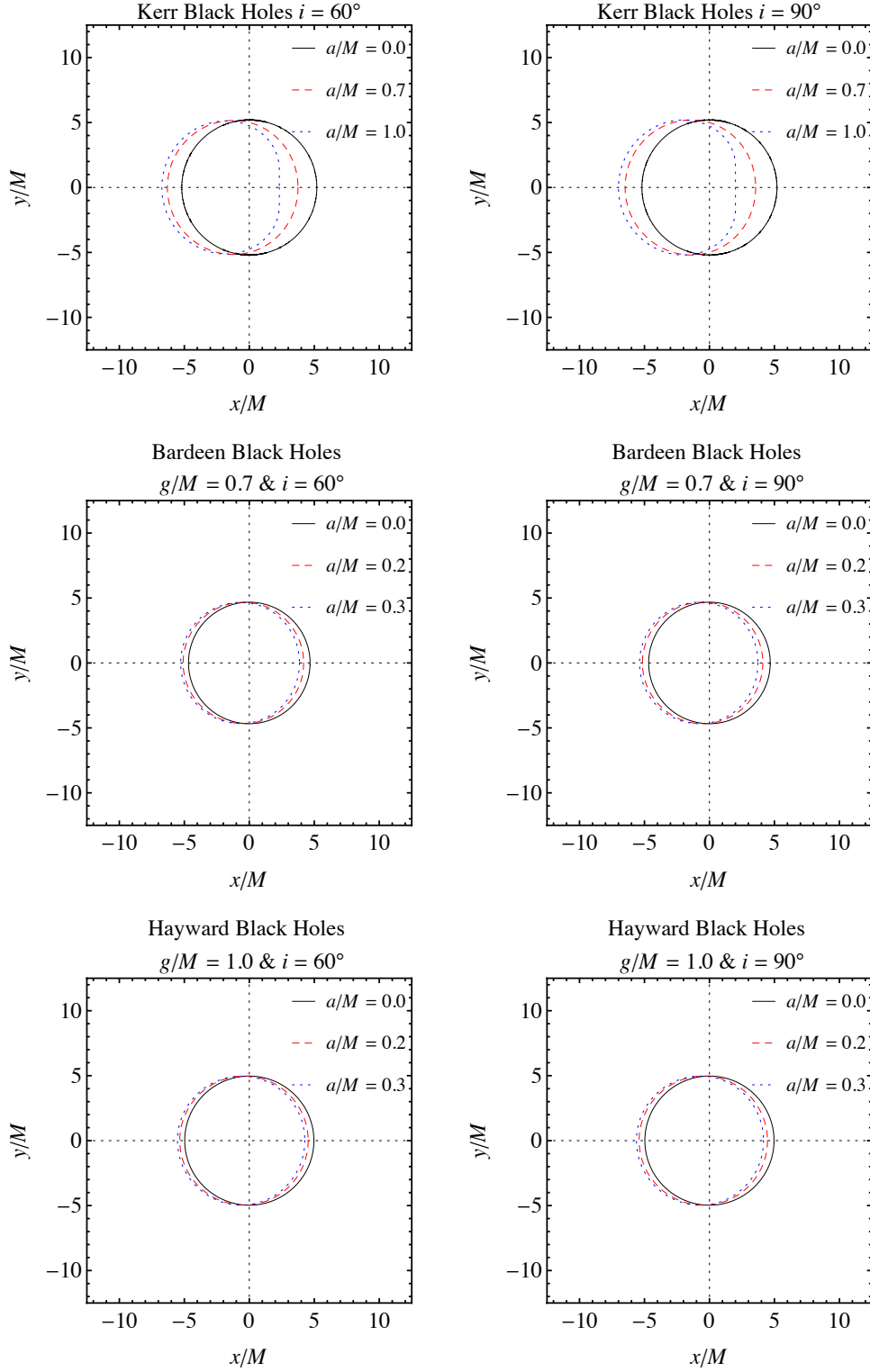


Figure 2. Some examples of boundary of shadow of Kerr BHs (top panels), Bardeen BHs (central panels), and Hayward BHs (bottom panels) for different values of the spin parameter a_* . The viewing angle is $i = 60^\circ$ (left panels) and 90° (right panels).

For a photon, the equation of motion for the radial coordinate r in Boyer-Lindquist coordinates is

$$\Sigma^2 \left(\frac{dr}{d\lambda} \right)^2 = \mathcal{R}, \quad (3.1)$$

where λ is an affine parameter, and

$$\mathcal{R} = E^2 r^4 + (a^2 E^2 - L_z^2 - \mathcal{Q}) r^2 + 2m[(aE - L_z)^2 + \mathcal{Q}]r - a^2 \mathcal{Q}, \quad (3.2)$$

$$\mathcal{Q} = p_\theta^2 + \cos^2 \theta \left(\frac{L_z^2}{\sin^2 \theta} - a^2 E^2 \right). \quad (3.3)$$

The parameter m in Eq. (3.2) is equal to: M , for a Kerr BH; m_B in Eq. (2.3) for a Bardeen BH; m_H in Eq. (2.4), for a Hayward BH. E , L_z , and \mathcal{Q} are constants of motion and are, respectively, the energy, the component of the angular momentum parallel to the BH spin, and the so-called Carter constant. p_θ is the canonical momentum conjugate to θ .

It is convenient to minimize the number of parameters by introducing the variables $\xi = L_z/E$ and $\eta = \mathcal{Q}/E^2$. ξ and η are very simply related to the so-called ‘‘celestial coordinates’’ x and y of the image, as seen by an observer at infinity who receives the light ray, by

$$x = \frac{\xi}{\sin i}, \quad y = \pm(\eta + a^2 \cos^2 i - \xi^2 \cot^2 i)^{1/2}, \quad (3.4)$$

where i is the angular coordinate of the observer at infinity. Precisely, x is the apparent perpendicular distance of the image from the axis of symmetry and y is the apparent perpendicular distance of the image from its projection on the equatorial plane.

The radial equation of motion (3.1) depends on θ only in the factor Σ^2 , and is decoupled from ϕ and t . Thus the behavior of $\mathcal{R}(r)$ determines the type of orbit and the question of escape versus plunge for given ξ and η . Since motion is only possible when $\mathcal{R}(r) \geq 0$, the analysis of the position of its roots (especially roots in $r \geq r_+$, where r_+ is the horizon) is a powerful method of investigation of photon orbits. Qualitatively, there are three kinds of photon orbits:

(i) $\mathcal{R}(r)$ may have no roots in $r \geq r_+$ (capture orbits), in which case the photon arrives from infinity and then crosses the horizon;

(ii) $\mathcal{R}(r)$ has real roots in $r \geq r_+$ (scattering orbits), in which case the motion of photon is described by null geodesics which have a turning point $\dot{r} = 0$;

(iii) unstable orbits of constant radius, which separate the capture and the scattering orbits, determined by

$$\mathcal{R}(r_*) = \frac{\partial \mathcal{R}}{\partial r}(r_*) = 0, \quad \text{and} \quad \frac{\partial^2 \mathcal{R}}{\partial r^2}(r_*) \geq 0, \quad (3.5)$$

with r_* being the greatest real root of \mathcal{R} .

The apparent shape of the BH can be found by looking for the unstable orbits. Every orbit can be characterized by the constants of motion ξ and η , and the set of unstable circular orbits (ξ_c, η_c) can be used to plot a closed curve in the xy plane which represents the boundary of the BH shadow. The apparent image of the BH is larger than its geometrical size, because the BH bends light rays and thus the actual cross section is larger than the geometrical one.

From Eqs. (3.2) and (3.5), the equations determining the unstable orbits of constant radius are

$$\begin{aligned}\mathcal{R} &= r^4 + (a^2 - \xi_c^2 - \eta_c)r^2 + 2m[\eta_c + (\xi_c - a)^2]r - a^2\eta_c = 0, \\ \frac{\partial\mathcal{R}}{\partial r} &= 4r^3 + 2(a^2 - \xi_c^2 - \eta_c)r + 2m[\eta_c + (\xi_c - a)^2] = 0.\end{aligned}\quad (3.6)$$

In the case of a Schwarzschild BH ($a = 0$ and $m = M$), the solution is [49]

$$\eta_c(\xi_c) = 27M^2 - \xi_c^2, \quad (3.7)$$

so the apparent image of the BH is a circle of radius $\sqrt{27}M$ (black solid circles in the left panels of Fig. 2). For a Kerr BH, one finds

$$\begin{aligned}\xi_c &= \frac{1}{a(r - M)}[M(r^2 - a^2) - r(r^2 - 2Mr + a^2)], \\ \eta_c &= \frac{r^3}{a^2(r - M)^2}[4a^2M - r(r - 3M)^2],\end{aligned}\quad (3.8)$$

where r is the radius of the unstable orbit. These two equations determine, parametrically, the critical locus (ξ_c, η_c) , which is the set of unstable circular orbits. The boundary of the shadows of Kerr BHs with $a/M = 0.0, 0.7$, and 1.0 are shown in Fig. 2 for an observer with angular coordinate $i = 60^\circ$ (top left panel) and for one on the equatorial plane (top right panel).

In the case of the Bardeen and Hayward BHs, the solutions are more complicated. Yet, we can solve Eq. (3.6) with $m = m_B$ and $m = m_H$, and obtain the formula of the critical locus (ξ_c, η_c) for these metrics. In Fig. 2, we show some examples of boundary of shadow of Bardeen BHs (central panels, with deformation parameter $g/M = 0.7$), and Hayward BHs (bottom panels, with deformation parameter $g/M = 1.0$) for $a_* = 0.0, 0.2$, and 0.3 . Such a low values of the spin parameter with respect to the Kerr case is motivated by the fact that the maximum value of a_* is lower than 1 for $g/M \neq 0$ and reduces to 0 for $g/M \approx 0.77$ (Bardeen) and 1.06 (Hayward). For higher values of the spin parameter, there is no horizon, and these metrics describe the gravitational field around unstable configurations of exotic matter.

4 Measuring the Kerr spin parameter from the black hole's shadow

In the observation of the shadow of a BH, it is helpful to introduce a parameter that approximately characterizes its shape [61]. At first approximation, the shape of the shadow of a BH is a circle, so we approximate the shadow by a circle passing through three points, which are located at the top position, the bottom position, and the most left end of its boundary (the three red points in the left panel of Fig. 3). The radius R_s of the shadow is hereby defined by the radius of this circle. On the other hand, when a BH rotates, the difference of the photon capture radius between co-rotating and counter-rotating particles introduces a dent on one side of the shadow. Unlike in the electromagnetic case, in gravity the spin-orbit interaction term is repulsive when the orbital angular momentum of the photon is parallel to the BH spin (the capture radius thus decreases), and attractive in the opposite case (the capture radius increases). The dent is more pronounced for fast-rotating objects and it is very clear for the case of an extremal Kerr BH and a large viewing angle i (the blue-dotted

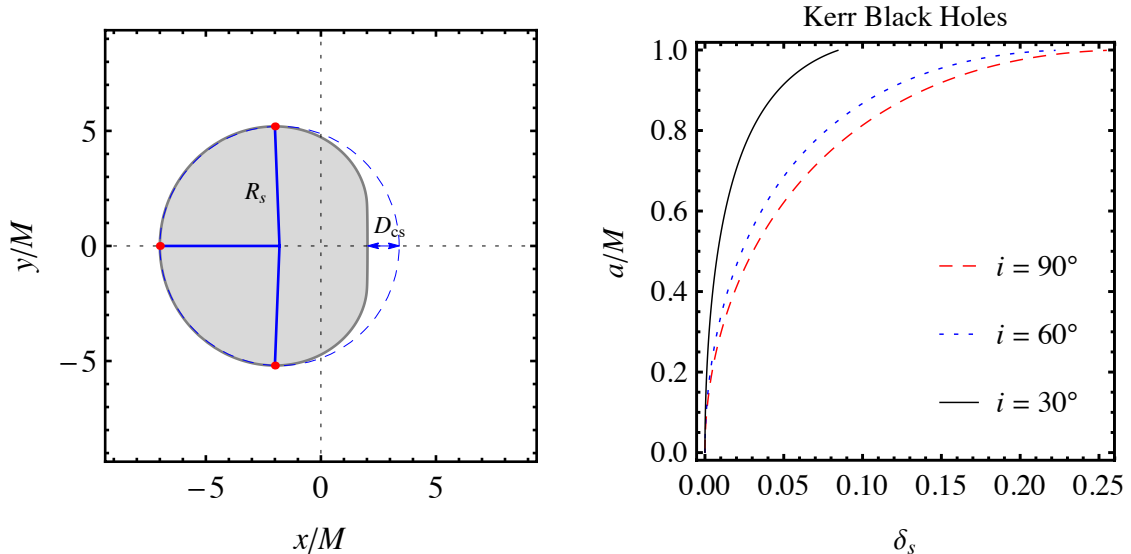


Figure 3. Left panel: BH’s shadow with the two parameters that approximately characterized its shape: the radius R_s (defined as the radius of the circle passing through the three red points located at the top, bottom, and most left end of the shadow) and the dent D_{cs} (the difference between the right endpoints of the circle and of the shadow). Right panel: Spin parameter $a_* = a/M$ as a function of the distortion parameter $\delta_s = D_{cs}/R_s$ for Kerr BHs and a viewing angle $i = 90^\circ$ (red dashed curve), 60° (blue dotted curve), and 30° (black solid curve).

curves in the left panels of Fig. 2). The size of the dent is evaluated by D_{cs} , which is the difference between the right endpoints of the circle and of the shadow (see the left panel of Fig. 3). Thus the distortion parameter δ_s of the shadow is defined by $\delta_s = D_{cs}/R_s$, which can be adopted as an observable in astronomical observations [61].

In the case of Kerr backgrounds, the exact shape of the shadow depends only on the BH spin parameter, a_* , and the line of sight of the distant observer with respect to the BH spin, i . For a given inclination angle i , there is a one-to-one correspondence between a_* and the distortion parameter δ_s . If we have an independent estimate of the viewing angle and we measure the distortion parameter of the shadow of a Kerr BH, we can infer its spin parameter a_* [61]. The right panel of Fig. 3 shows the curves describing the spin parameter $a_* = a/M$ as a function of the distortion parameter δ_s for Kerr BHs and an inclination angle $i = 90^\circ$ (red dashed curve), 60° (blue dotted curve), and 30° (black solid curve).

The same idea can be applied to non-Kerr BHs. If we consider the Bardeen and Hayward BHs with a specific value of the deformation parameter g/M , for a given inclination angle i there is a one-to-one correspondence between the spin a_* and the distortion parameter δ_s . The counterpart of the right panel in Fig. 3 for the Bardeen and Hayward BHs are shown, respectively, in Fig. 4 and Fig. 5 for several values of g/M . The relation between a_* and δ_s depends on g/M and it reduces to the Kerr one for $g = 0$.

As in Ref. [31], we can now address the question of what happens if we measure the Kerr spin parameter of a non-Kerr BH; that is, we estimate the spin parameter a_* from the measurement of the distortion parameter δ_s of the shadow of a Bardeen or Hayward BH assuming it is of Kerr type. In the Kerr metric, there is a one-to-one correspondence between the spin parameter and δ_s and therefore, from the measurement of the latter, we can infer

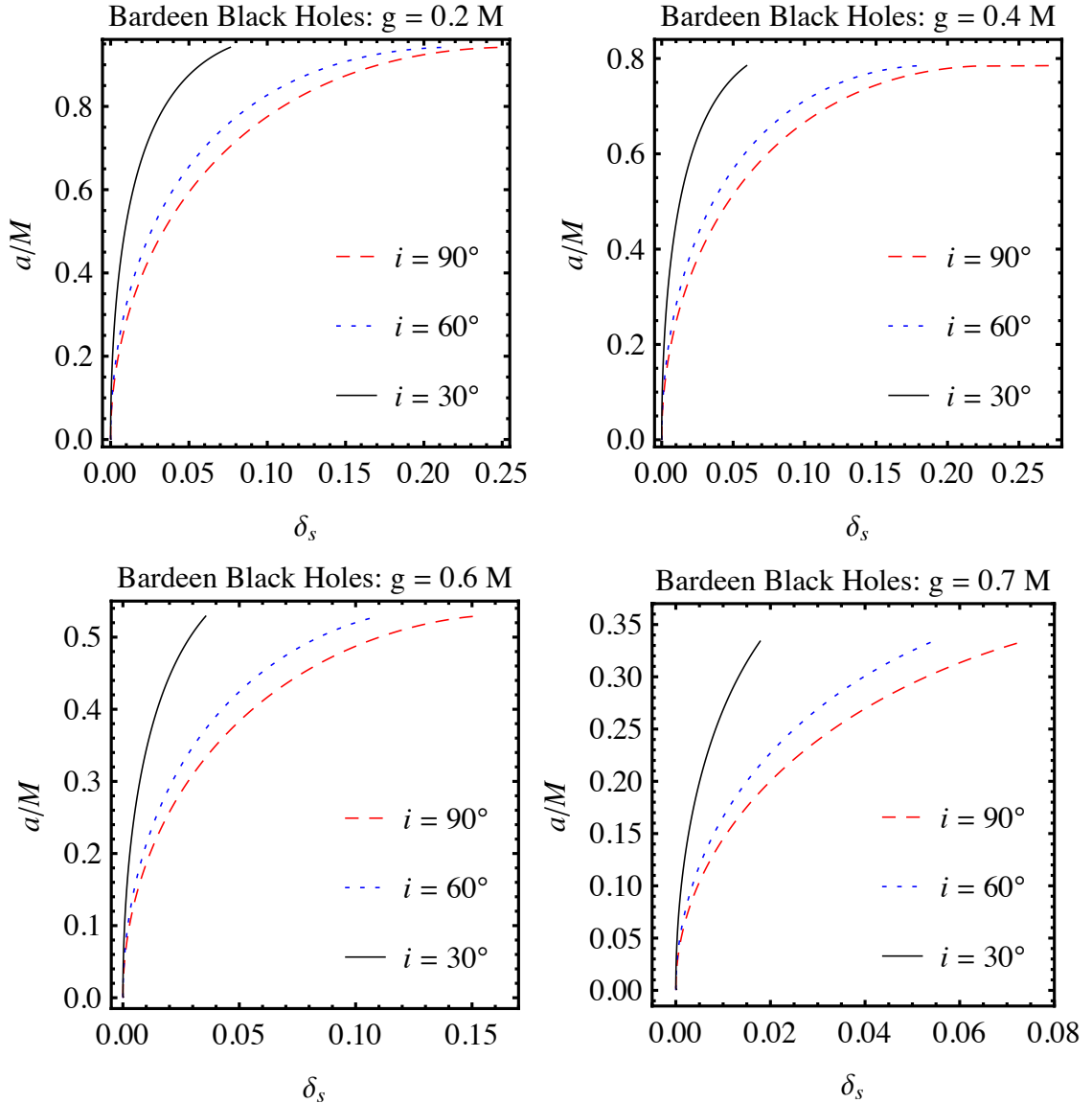


Figure 4. As in the right panel of Fig. 3 for the case of Bardeen BHs with $g/M = 0.2$ (top left panel), 0.4 (top right panel), 0.6 (bottom left panel), and 0.7 (bottom right panel).

the Kerr spin from

$$a_*^{\text{Kerr}} = a_*^{\text{Kerr}}(\delta_s). \quad (4.1)$$

However, in the Bardeen (and Hayward) background the distortion parameter is given by $\delta_s(a_*^{\text{B}}, g/M)$ and therefore the Kerr spin parameter of a Bardeen BH with spin a_*^{B} and charge g/M is

$$a_*^{\text{Kerr}} = a_*^{\text{Kerr}}[\delta_s(a_*^{\text{B}}, g/M)]. \quad (4.2)$$

The result of a similar measurement is reported in Figs. 6 and 7 for the case of Bardeen BHs, and in Fig. 8 for Hayward BHs. The result is independent of the inclination angle i . For

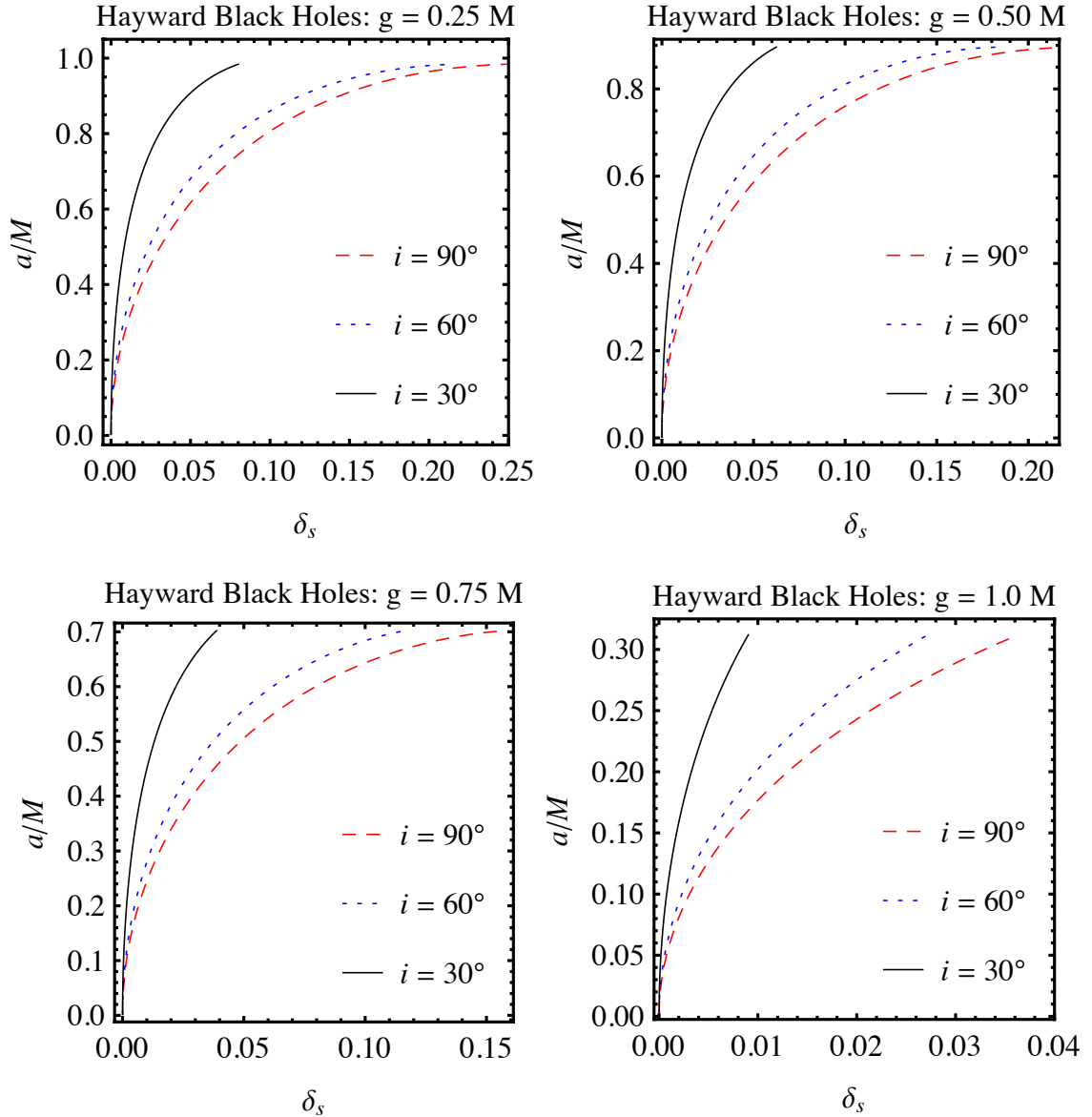


Figure 5. As in the right panel of Fig. 3 for the case of Hayward BHs with $g/M = 0.25$ (top left panel), 0.50 (top right panel), 0.75 (bottom left panel), and 1.00 (bottom right panel).

non-rotating objects, this approach trivially provides the correct spin: for any spherically symmetric BH, the shadow is always a circle, $\delta_s = 0$, independently of possible deviations from the Kerr background. For slow-rotating BHs, we find a discrepancy between the actual spin parameter of the compact object and the one inferred assuming a Kerr metric. Such a difference increases for higher values of a_* and it can be quite significant for large values of g/M .

5 Discussion

The distortion parameter δ_s is just a number and therefore cannot determine both the exact spin a_* and the deformation g/M . However, it is remarkable that the shadow of a regular

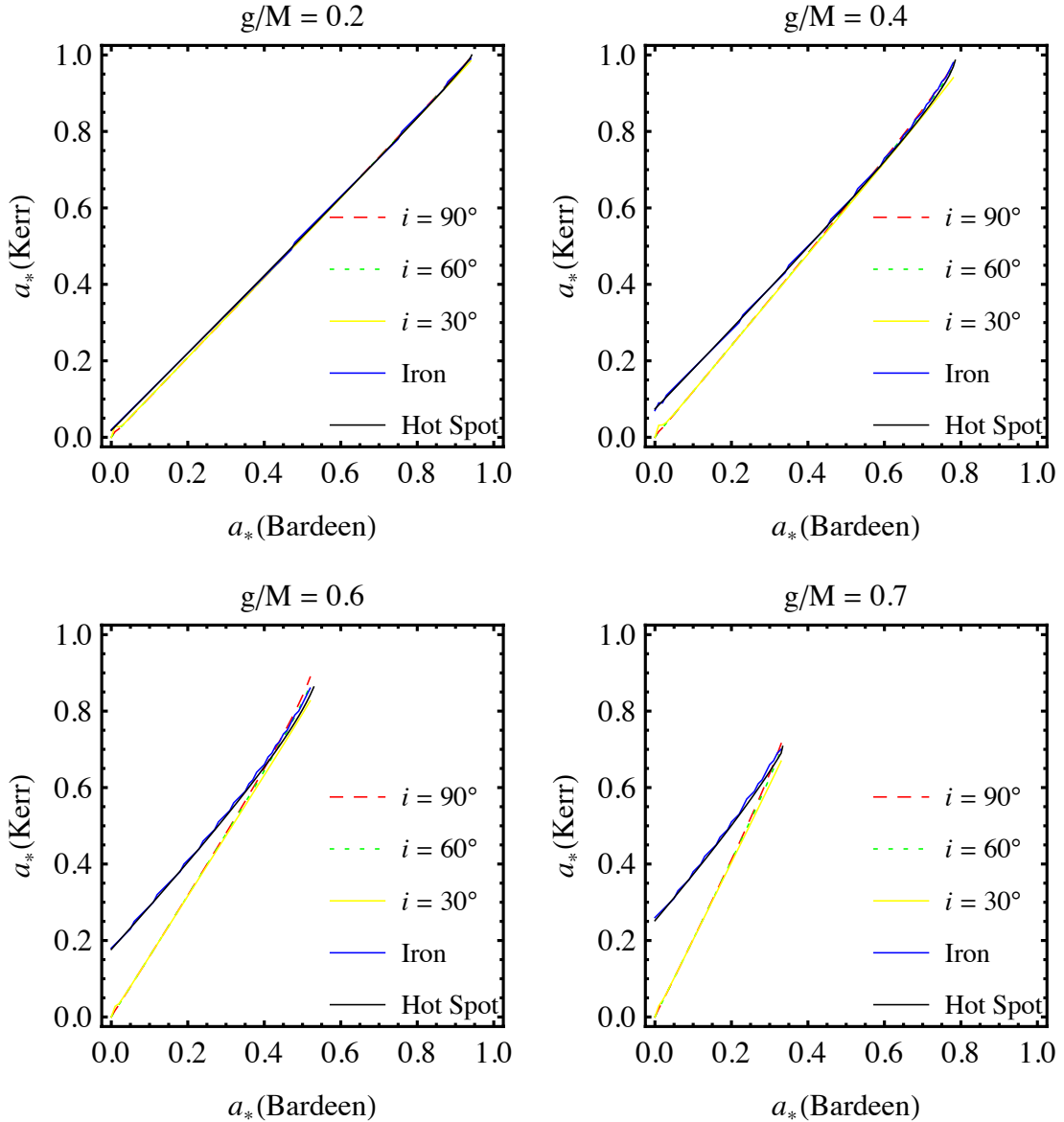


Figure 6. Spin parameter of a Bardeen BH, $a_*(\text{Bardeen})$, against the spin parameter that one would infer for this object assuming the Kerr background, $a_*(\text{Kerr})$, through the determination of the distortion parameter of the shadow δ_s (red dashed curve, dotted green curve, and yellow solid curve respectively for a viewing angle $i = 90^\circ$, 60° , and 30°), the analysis of the $K\alpha$ iron line (blue solid curve), and the frequency of a test-particle at the ISCO radius (hot spot model, black solid curve). $g/M = 0.2$ (top left panel), 0.4 (top right panel), 0.6 (bottom left panel), and 0.7 (bottom right panel). See the text for more details.

BH with a large g/M cannot mimic the one of a fast-rotating Kerr BH. In other words, if we observe a shadow that looks like the one of a Kerr BH with high spin, we can constrain the deformation parameter g/M . In general, this is not possible, and we should combine this measurement with an independent one, in order to break the degeneracy between a_* and g/M .

In Ref. [31], one of us has shown that the simultaneous measurement of the Kerr spin via

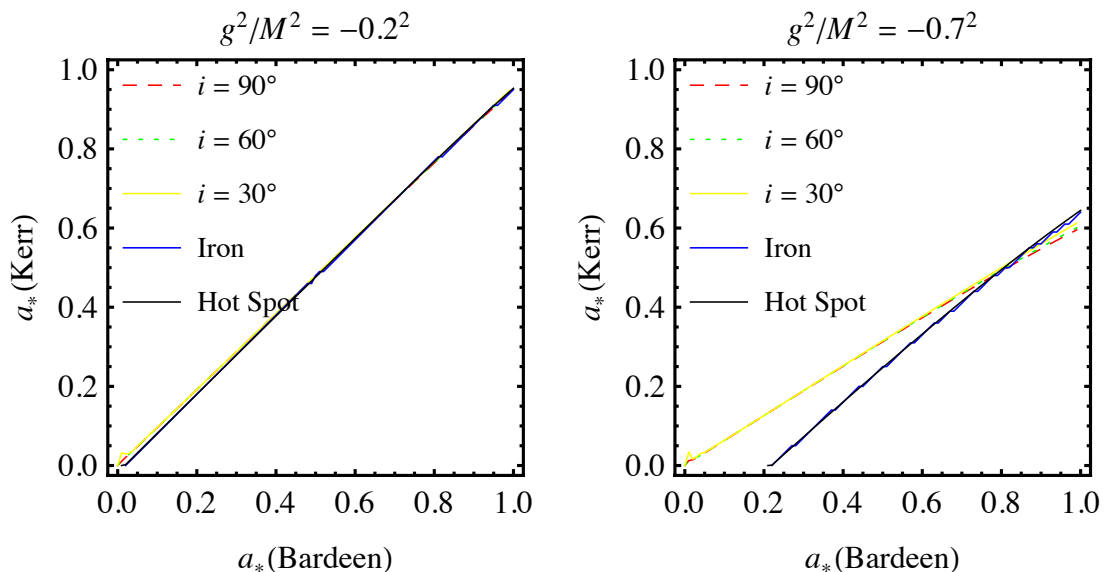


Figure 7. As in Fig. 6 for $(g/M)^2 = -(0.2)^2$ (left panel) and $-(0.7)^2$ (right panel).

the continuum-fitting and the iron line methods cannot fix this problem for Bardeen BHs. The two techniques provide the same information on the geometry of the spacetime around the compact object. We can now check if the combination of the Kerr spin parameter measured with the shadow approach can be combined with another estimate and if it is possible to distinguish a true Kerr BH from a Bardeen or Hayward one. Near future VLBI facilities will be able to image only the shadow of super-massive BH candidates. The analysis of the $K\alpha$ iron line is currently the only technique that can provide a relatively robust estimate of the Kerr spin parameter of these objects (the continuum-fitting method can be used only for stellar-mass BH candidates). It is supposed that VLBI experiments will be able to observe also hot blobs of plasma orbiting around nearby super-massive BH candidates and infer their angular frequency at the ISCO radius. Such a time measurement can provide an independent measurement of the Kerr spin parameter, as in the Kerr metric there is a one-to-one correspondence between BH spin and angular frequency of the ISCO.

The profile of the $K\alpha$ iron line depends on the background metric, the geometry of the emitting region, the disk emissivity, and the disk's inclination angle with respect to the line of sight of the distant observer. In the Kerr spacetime, the only relevant parameter of the background geometry is the spin parameter a_* , while M sets the length of the system, without affecting the shape of the line. In those sources for which there is indication that the line is mainly emitted close to the compact object, the emission region may be thought to range from the radius of the ISCO, $r_{\text{in}} = r_{\text{ISCO}}$, to some outer radius r_{out} . In principle, the disk emissivity could be theoretically calculated. In practice, that is not feasible at present. The simplest choice is an intensity profile $I_e \propto r^\alpha$ with index $\alpha < 0$ to be determined during the fitting procedure. The fourth parameter is the inclination of the disk with respect to the line of sight of the distant observer, i . The dependence of the line profile on a_* , i , α , and r_{out} in the Kerr background has been analyzed in detail by many authors, starting with Ref. [20]. In the case of non-Kerr backgrounds, see e.g. Ref. [27].

The profile of the $K\alpha$ iron line can be obtained by computing the photon flux number

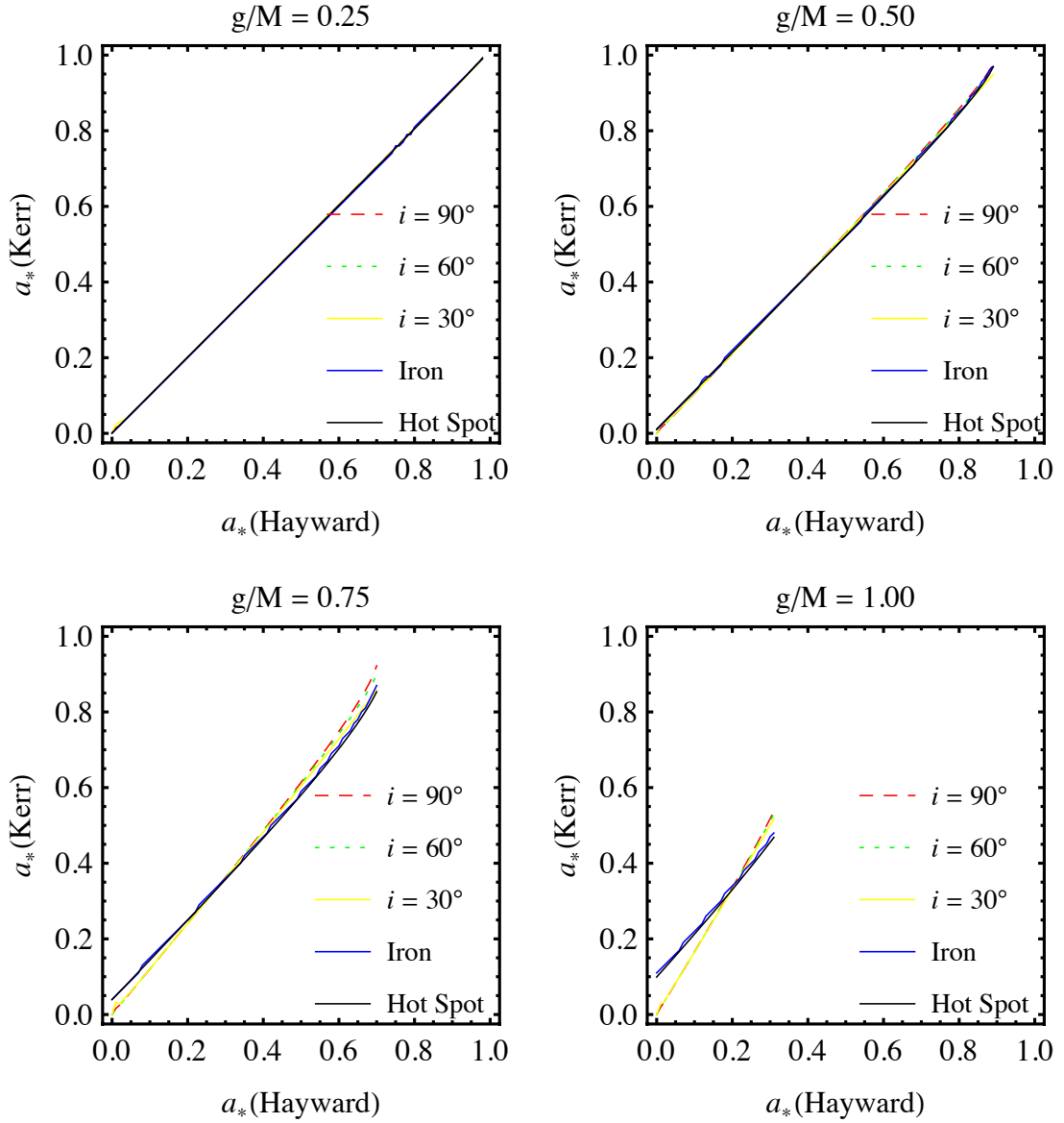


Figure 8. As in Fig. 6 for Hayward BHs with $g/M = 0.25$ (top left panel), 0.50 (top right panel), 0.75 (bottom left panel), and 1.00 (bottom right panel).

density measured by a distant observer, that is

$$N_{E_{\text{obs}}} = \frac{1}{E_{\text{obs}}} \int I_{\text{obs}}(E_{\text{obs}}) d\Omega_{\text{obs}} = \frac{1}{E_{\text{obs}}} \int w^3 I_e(E_e) d\Omega_{\text{obs}}, \quad (5.1)$$

where I_{obs} and E_{obs} are, respectively, the specific intensity of the radiation and the photon energy as measured by the distant observer, while I_e and E_e are the same quantities in the rest-frame of the emitter. $d\Omega_{\text{obs}}$ is the solid angle seen by the distant observer and w is the redshift factor

$$w = \frac{E_{\text{obs}}}{E_e} = \frac{k_\alpha u_{\text{obs}}^\alpha}{k_\beta u_e^\beta}. \quad (5.2)$$

Here k^α is the 4-momentum of the photon, $u_{\text{obs}}^\alpha = (-1, 0, 0, 0)$ is the 4-velocity of the distant observer, and $u_e^\alpha = (u_e^t, 0, 0, \Omega u_e^t)$ is the 4-velocity of the emitter. Ω is the angular velocity for equatorial circular orbits. $I_e(E_e)/E_e^3 = I_{\text{obs}}(E_{\text{obs}})/E_{\text{obs}}^3$ follows from the Liouville's theorem. Using the normalization condition $g_{\mu\nu}u_e^\mu u_e^\nu = -1$, one finds

$$u_e^t = -\frac{1}{\sqrt{-g_{tt} - 2g_{t\phi}\Omega - g_{\phi\phi}\Omega^2}}. \quad (5.3)$$

The redshift factor is thus given by

$$w = \frac{\sqrt{-g_{tt} - 2g_{t\phi}\Omega - g_{\phi\phi}\Omega^2}}{1 + \lambda\Omega}, \quad (5.4)$$

where $\lambda = k_\phi/k_t$ is a constant of the motion along the photon path. Doppler boosting, gravitational redshift, and frame dragging are entirely encoded in the redshift factor w . As the $K\alpha$ iron line is intrinsically narrow in frequency, we can assume that the disk emission is monochromatic (the rest frame energy is $E_{K\alpha} = 6.4$ keV) and isotropic with a power-law radial profile:

$$I_e(E_e) \propto \delta(E_e - E_{K\alpha})r^\alpha. \quad (5.5)$$

Let us now consider the possibility that an astrophysical BH candidate is a Bardeen BH and that we want to measure the spin parameter of this object with the $K\alpha$ iron line analysis, assuming that the object is a Kerr BH. In this case, we can use an approach similar to the one discussed in Ref. [27] and define the reduced χ^2 :

$$\chi_{\text{red}}^2(a_*^{\text{Kerr}}, i) = \frac{1}{n} \sum_{i=1}^n \frac{[N_i^{\text{Kerr}}(a_*^{\text{Kerr}}, i) - N_i^{\text{B}}(a_*^{\text{B}}, g/M, i^{\text{B}})]^2}{\sigma_i^2}, \quad (5.6)$$

where the summation is performed over n sampling energies E_i and N_i^{Kerr} and N_i^{B} are the normalized photon fluxes in the energy bin $[E_i, E_i + \Delta E]$, respectively for the Kerr and the Bardeen metric. The error σ_i is assumed to be 15% the photon flux N_i^{B} , which is roughly the accuracy of current observations in the best situations. In this paper, all the calculations are done with an intensity profile index $\alpha = -3$ and an outer radius $r_{\text{out}} = r_{\text{in}} + 100 M$. For specific values of a_*^{B} and g/M , we can find the minimum of the reduced χ^2 , and we thus obtain what we call the Kerr spin parameter.

In the case of the frequency of a hot spot at the ISCO radius, the idea is the same. In the Kerr background, there is a one-to-one correspondence between Ω_{ISCO} and a_* , so we can write $\Omega_{\text{ISCO}}^{\text{Kerr}}(a_*^{\text{Kerr}})$ and the inverse function $a_*^{\text{Kerr}}(\Omega_{\text{ISCO}}^{\text{Kerr}})$. In the Bardeen (and Hayward) background the frequency at the ISCO radius depends on both the spin a_*^{B} and the deformation parameter g/M , so $\Omega_{\text{ISCO}}^{\text{B}}(a_*^{\text{B}}, g/M)$. If we measure the frequency of a hot spot at the ISCO radius and we assume that the object is a Kerr BH, while it is of Bardeen type, one finds:

$$a_*^{\text{Kerr}} = a_*^{\text{Kerr}}[\Omega_{\text{ISCO}}^{\text{B}}(a_*^{\text{B}}, g/M)], \quad (5.7)$$

which is the Kerr spin parameter of the Bardeen BH.

Figs. 6-8 show also the possible measurements of the Kerr spin parameter with these two techniques (blue solid line for the iron line, black solid line for the hot spot). First, it seems

like the iron line and hot spot approaches provide essentially the same result. This is because the two techniques are essentially sensitive to the properties at the ISCO radius. Second, when we compare the results of these approaches with the measurements inferred from the shadow, we see that the measurements disagree in the case of non-rotating BHs, while the discrepancy decreases as the spin parameter increases and there is almost no difference for near extremal states. So, the determination of the distortion parameter of the shadow of a BH candidate can potentially test the nature of the compact object when combined with the iron line analysis or the hot spot approach for non-rotating or slow-rotating objects. The degeneracy between a_* and g/M cannot be solved in the case of near extremal BHs, which confirms the difficulties, found in Ref. [31], to test this kind of non-Kerr metrics. Lastly, let us notice that here we have always considering an “ideal” observation, neglecting possible uncertainty in the measurements. We thus adopt an optimistic point of view, and the difficulties to measure deviations from the Kerr solution are even more challenging.

6 Summary and conclusions

Astrophysical BH candidates are thought to be the Kerr BHs of general relativity, but the actual nature of these objects is still to be verified. The analysis of the thermal spectrum of thin accretion disks and of the profile of the $K\alpha$ iron line are today the only available approaches to probe the spacetime geometry around BH candidates and test the Kerr BH hypothesis. However, there is a strong correlation between the spin parameter and possible deviations from the Kerr solution and it is not possible to check the nature of a specific source with a single measurement. As shown in Ref. [31], at least for some non-Kerr metrics, the disk’s thermal spectrum and the iron line provide essentially the same information. So, the two measurements may be consistent with the ones of a Kerr BH with a certain value of the spin parameter a_* even if the object is actually something else with a different spin. The combination of the two measurements does not break the degeneracy.

In this paper, we have investigated the possibility of measuring the Kerr spin parameter from the BH shadow. Near future mm/sub-mm VLBI facilities will be able to observe the emitting region around nearby super-massive BH candidates with a resolution comparable to their gravitational radius. If the gas is geometrically thick and optically thin, we will observe a dark area over a brighter background. While the intensity map of this image depends on the kind of accretion process and the emission mechanisms, the boundary of the shadow is completely determined by the geometry of the spacetime. The shape of the shadow is expected to be a circle for non-rotating BHs or a viewing angle $i = 0^\circ$ or 180° , and slightly deformed otherwise, as a consequence of the coupling between the spin of the compact object and the photon angular momentum. Such a deformation can be measured in terms of the distortion parameter δ_s , which, in turn, may provide an estimate of the spin parameter a_* .

If the compact object is not a Kerr BH, but we assume it is, this technique still provides the correct value of a_* for non-rotating objects, but a wrong measurement for near extremal states. We have compared these measurements with the ones of the spin that one could infer from the iron line and from the determination of the frequency at the ISCO radius (a kind of measurement that should become possible and reliable with VLBI facilities). For non-rotating BHs, the shadow approach would provide a different result, so the possible inconsistency between two measurements may be an indication of deviations from the Kerr solution. All the approaches converge instead to the same value for near extremal BHs. This work thus confirm the intrinsic difficulty to test the Kerr-nature of astrophysical BH

candidates, even with future facilities. It may however be possible that good measurements of the shadow, in which one can extract more than one parameter characterizing the shape, are able to break the degeneracy between the spin and possible deviations from the Kerr geometry for any value of a_* .

Acknowledgments

This work was supported by the NSFC grant No. 11305038, the Shanghai Municipal Education Commission grant for Innovative Programs No. 14ZZ001, the Thousand Young Talents Program, and Fudan University.

References

- [1] B. Carter, Phys. Rev. Lett. **26**, 331 (1971).
- [2] D. C. Robinson, Phys. Rev. Lett. **34**, 905 (1975).
- [3] P. T. Chrusciel, J. L. Costa and M. Heusler, Living Rev. Rel. **15**, 7 (2012) [arXiv:1205.6112 [gr-qc]].
- [4] R. H. Price, Phys. Rev. D **5**, 2419 (1972).
- [5] R. H. Price, Phys. Rev. D **5**, 2439 (1972).
- [6] C. Bambi, A. D. Dolgov and A. A. Petrov, JCAP **0909**, 013 (2009) [arXiv:0806.3440 [astro-ph]].
- [7] R. Narayan, New J. Phys. **7**, 199 (2005) [gr-qc/0506078].
- [8] C. E. Rhoades and R. Ruffini, Phys. Rev. Lett. **32**, 324 (1974).
- [9] V. Kalogera and G. Baym, Astrophys. J. **470**, L61 (1996).
- [10] E. Maoz, Astrophys. J. **494**, L181 (1998) [astro-ph/9710309].
- [11] R. Narayan and J. E. McClintock, New Astron. Rev. **51**, 733 (2008) [arXiv:0803.0322 [astro-ph]].
- [12] A. E. Broderick, A. Loeb and R. Narayan, Astrophys. J. **701**, 1357 (2009) [arXiv:0903.1105 [astro-ph.HE]].
- [13] M. A. Abramowicz, W. Kluzniak and J. -P. Lasota, Astron. Astrophys. **396**, L31 (2002) [astro-ph/0207270].
- [14] C. Bambi, The Scientific World Journal **2013**, 204315 (2013) [arXiv:1205.4640 [gr-qc]].
- [15] C. Bambi, Mod. Phys. Lett. A **26**, 2453 (2011) [arXiv:1109.4256 [gr-qc]].
- [16] C. Bambi, Astron. Rev. **8**, 4 (2013) [arXiv:1301.0361 [gr-qc]].
- [17] S. N. Zhang, W. Cui and W. Chen, Astrophys. J. **482**, L155 (1997) [astro-ph/9704072].
- [18] L. -X. Li, E. R. Zimmerman, R. Narayan and J. E. McClintock, Astrophys. J. Suppl. **157**, 335 (2005) [astro-ph/0411583].
- [19] J. E. McClintock, R. Narayan, S. W. Davis, L. Gou, A. Kulkarni, J. A. Orosz, R. F. Penna and R. A. Remillard *et al.*, Class. Quant. Grav. **28**, 114009 (2011) [arXiv:1101.0811 [astro-ph.HE]].
- [20] A. C. Fabian, M. J. Rees, L. Stella and N. E. White, Mon. Not. Roy. Astron. Soc. **238**, 729 (1989).
- [21] A. C. Fabian, K. Iwasawa, C. S. Reynolds and A. J. Young, Publ. Astron. Soc. Pac. **112**, 1145 (2000) [astro-ph/0004366].
- [22] C. S. Reynolds and M. A. Nowak, Phys. Rept. **377**, 389 (2003) [astro-ph/0212065].

- [23] D. F. Torres, Nucl. Phys. B **626**, 377 (2002) [hep-ph/0201154].
- [24] Y. Lu and D. F. Torres, Int. J. Mod. Phys. D **12**, 63 (2003) [astro-ph/0205418].
- [25] C. Bambi and E. Barausse, Astrophys. J. **731**, 121 (2011) [arXiv:1012.2007 [gr-qc]].
- [26] C. Bambi, Astrophys. J. **761**, 174 (2012) [arXiv:1210.5679 [gr-qc]].
- [27] C. Bambi, Phys. Rev. D **87**, 023007 (2013) [arXiv:1211.2513 [gr-qc]].
- [28] C. Bambi, Phys. Rev. D **87**, 084039 (2013) [arXiv:1303.0624 [gr-qc]].
- [29] C. Bambi and D. Malafarina, Phys. Rev. D **88**, 064022 (2013) [arXiv:1307.2106 [gr-qc]].
- [30] C. Bambi, arXiv:1308.2470 [gr-qc].
- [31] C. Bambi, JCAP **1308**, 055 (2013) [arXiv:1305.5409 [gr-qc]].
- [32] T. Johannsen and D. Psaltis, Astrophys. J. **726**, 11 (2011) [arXiv:1010.1000 [astro-ph.HE]].
- [33] C. Bambi, JCAP **1209**, 014 (2012) [arXiv:1205.6348 [gr-qc]].
- [34] F. D. Ryan, Phys. Rev. D **52**, 5707 (1995).
- [35] N. Wex and S. Kopeikin, Astrophys. J. **514**, 388 (1999) [astro-ph/9811052].
- [36] K. Glampedakis and S. Babak, Class. Quant. Grav. **23**, 4167 (2006) [arXiv:gr-qc/0510057].
- [37] L. Barack and C. Cutler, Phys. Rev. D **75**, 042003 (2007) [arXiv:gr-qc/0612029].
- [38] T. A. Apostolatos, G. Lukes-Gerakopoulos and G. Contopoulos, Phys. Rev. Lett. **103**, 111101 (2009) [arXiv:0906.0093 [gr-qc]].
- [39] G. Lukes-Gerakopoulos, T. A. Apostolatos and G. Contopoulos, Phys. Rev. D **81**, 124005 (2010) [arXiv:1003.3120 [gr-qc]].
- [40] C. Bambi and G. Lukes-Gerakopoulos, Phys. Rev. D **87**, 083006 (2013) [arXiv:1302.0565 [gr-qc]].
- [41] C. Bambi, Phys. Rev. D **85**, 043002 (2012) [arXiv:1201.1638 [gr-qc]].
- [42] C. Bambi, Phys. Rev. D **86**, 123013 (2012) [arXiv:1204.6395 [gr-qc]].
- [43] C. Bambi, Phys. Rev. D **83**, 103003 (2011) [arXiv:1102.0616 [gr-qc]].
- [44] C. Bambi, Phys. Lett. B **705**, 5 (2011) [arXiv:1110.0687 [gr-qc]].
- [45] C. Bambi, Phys. Rev. D **85**, 043001 (2012) [arXiv:1112.4663 [gr-qc]].
- [46] Z. Li and C. Bambi, JCAP **1303**, 031 (2013) [arXiv:1212.5848 [gr-qc]].
- [47] S. Doeleman, J. Weintroub, A. E. E. Rogers, R. Plambeck, R. Freund, R. P. J. Tilanus, P. Friberg and L. M. Ziurys *et al.*, Nature **455**, 78 (2008) [arXiv:0809.2442 [astro-ph]].
- [48] S. Doeleman, E. Agol, D. Backer, F. Baganoff, G. C. Bower, A. Broderick, A. Fabian and V. Fish *et al.*, arXiv:0906.3899 [astro-ph.CO].
- [49] S. Chandrasekhar, *The Mathematical Theory of Black Holes* (Clarendon Press, Oxford, UK, 1983).
- [50] H. Falcke, F. Melia and E. Agol, Astrophys. J. **528**, L13 (2000) [astro-ph/9912263].
- [51] R. Takahashi, J. Korean Phys. Soc. **45**, S1808 (2004) [Astrophys. J. **611**, 996 (2004)] [astro-ph/0405099].
- [52] C. Bambi and K. Freese, Phys. Rev. D **79**, 043002 (2009) [arXiv:0812.1328 [astro-ph]].
- [53] C. Bambi, K. Freese and R. Takahashi, in *Windows on the Universe*, edited by L. Celnikier et al. (The Gioi Publishers, Ha Noi, Vietnam, 2010), pp. 575-578 [arXiv:0908.3238 [astro-ph.HE]].
- [54] C. Bambi and N. Yoshida, Class. Quant. Grav. **27**, 205006 (2010) [arXiv:1004.3149 [gr-qc]].

- [55] L. Amarilla, E. F. Eiroa and G. Giribet, Phys. Rev. D **81**, 124045 (2010) [arXiv:1005.0607 [gr-qc]].
- [56] T. Johannsen and D. Psaltis, Astrophys. J. **718**, 446 (2010) [arXiv:1005.1931 [astro-ph.HE]].
- [57] C. Bambi, F. Caravelli and L. Modesto, Phys. Lett. B **711**, 10 (2012) [arXiv:1110.2768 [gr-qc]].
- [58] L. Amarilla and E. F. Eiroa, Phys. Rev. D **85**, 064019 (2012) [arXiv:1112.6349 [gr-qc]].
- [59] L. Amarilla and E. F. Eiroa, Phys. Rev. D **87**, 044057 (2013) [arXiv:1301.0532 [gr-qc]].
- [60] C. Bambi, Phys. Rev. D **87**, 107501 (2013) [arXiv:1304.5691 [gr-qc]].
- [61] K. Hioki and K. -i. Maeda, Phys. Rev. D **80**, 024042 (2009) [arXiv:0904.3575 [astro-ph.HE]].
- [62] E. Ayon-Beato and A. Garcia, Phys. Lett. B **493**, 149 (2000) [gr-qc/0009077].
- [63] S. A. Hayward, Phys. Rev. Lett. **96**, 031103 (2006) [gr-qc/0506126].
- [64] C. Bambi and L. Modesto, Phys. Lett. B **721**, 329 (2013) [arXiv:1302.6075 [gr-qc]].
- [65] Z. Li and C. Bambi, Phys. Rev. D **87**, 124022 (2013) [arXiv:1304.6592 [gr-qc]].
- [66] P. J. Young, Phys. Rev. D **14**, 3281 (1976).